SFB/CPP-09-116
TTP09-43

Finite top quark mass effects in NNLO Higgs boson production at LHC

Alexey Pak, Mikhail Rogal, Matthias Steinhauser
Institut für Theoretische Teilchenphysik
Karlsruhe Institute of Technology (KIT)
76128 Karlsruhe, Germany

Abstract

We present next-to-next-to-leading order corrections to the inclusive production of the Higgs bosons at the CERN Large Hadron Collider (LHC) including finite top quark mass effects. Expanding our analytic results for the partonic cross section around the soft limit we find agreement with a very recent publication by Harlander and Ozeren [1].

PACS numbers: 12.38.Bx 14.80.Bn

1 Introduction

With the launch of the Large Hadron Collider (LHC) at CERN the particle physics experiments enter a new energy domain with the hope to discover new phenomena. Experimental observations are expected to provide hints for the still open questions within the Standard Model. Among these questions is the mechanism of the electroweak symmetry breaking which in most practical theories provides masses to the particles. The traditional implementation of the symmetry breaking implies the existence of a new particle, the Higgs boson, which so far has not been detected in high-energy collisions.

For the intermediate Higgs boson mass, favoured by the results of indirect searches, the most important production channel at a hadron collider is gluon fusion, $gg \to H$, mediated by a top quark loop. During the last 20 years enormous efforts have been made to evaluate higher order corrections to this process.

The leading order (LO) result has been presented in Refs. [2–5] and already almost 15 years ago also the next-to-leading order (NLO) QCD corrections became available [6, 7]. More recently also the next-to-next-to-leading order (NNLO) corrections have been evaluated [8–11]. While the NLO results are exact in the top quark and Higgs boson masses (in this context, see also Ref. [12]), the NNLO results rely on the effective theory built in the limit of the large top quark mass (see, e.g., Refs. [13, 14] for the three-loop corrections to the effective ggH coupling). It is well known that this approximation works surprisingly well at NLO, leading to deviations from the exact result that are less than 2% for $M_H < 2M_t$ [15]. It is one of the aims of the present paper to investigate the validity of the large top quark mass approximation at NNLO.

During the last few years there appeared several improvements over the fixed-order calculation. Among them is the soft-gluon resummation to next-to-next-to-leading [16] and next-to-next-to-next-to-leading [17] logarithmic orders and the identification (and resummation) of certain π^2 terms [18] which significantly improves the perturbative series. We furthermore want to mention Ref. [19] where the gluon-gluon channel has been considered in the limit of large center-of-mass energy $\sqrt{\hat{s}}$. Recent numerical predictions of Higgs boson production in gluon fusion both at the Tevatron and the LHC are summarized in Ref. [20].

Very recently the effects of the finite top quark mass on the Higgs boson production in hadron colliders have been reported in Ref. [1]. The authors of that reference carried out an asymptotic expansion of the corresponding production diagrams and obtained results for the first four terms in the $\rho = M_H^2/M_t^2$ expansion, where the secondary expansion around the soft limit (i.e. for $x = M_H^2/\hat{s} \to 1$) has been performed to a sufficiently high order.

In this paper we present the results of an independent calculation of these finite top mass effects, confirming the conclusions of Ref. [1]. Similarly to Ref. [1], we apply asymptotic expansion in $1/M_t$ to the full QCD diagrams and evaluate a few first terms of the series. However, our results are not expanded near the soft limit and the x-dependence of the cross section (which is valid below the top pair threshold, as discussed further) is retained.

The remainder of the paper is organized as follows. In the next Section we discuss the cross sections in the individual channels of partonic reactions at NLO and NNLO. We consider in particular the behaviour near $x \to 0$ and describe a method to extrapolate our results to the limit of large $\hat{s}$. In Section 3 we use the results of Section 2 and numerically evaluate the hadronic cross section for the LHC and the Tevatron. Our conclusions are presented in Section 4.

2 Partonic cross section

2.1 Notations and calculation details

We introduce the following notation for the partonic cross section:

$$\hat{\sigma}_{ij\to H+X} = \hat{A}_{\rm LO} \left(\Delta_{ij}^{(0)} + \frac{\alpha_s}{\pi} \Delta_{ij}^{(1)} + \left(\frac{\alpha_s}{\pi}\right)^2 \Delta_{ij}^{(2)} + \ldots \right) , \tag{1}$$

with

$$\hat{A}_{\rm LO} = \frac{G_F \, \alpha_s^2}{288\sqrt{2}\pi} f_0(\rho, 0) \tag{2}$$

and ij denoting one of the possible initial states: gg, qg, $q\bar{q}$, qq, or qq', where q and q' stand for (different) massless quark flavours.[1] At NNLO the Higgs boson in the final state may be accompanied by zero, one or two gluons, or by a light quark pair. In general, the quantities $\Delta_{ij}^{(k)}$ depend on x and ρ. Leading order mass dependence is then described by the function $f_0(\rho, 0)$ given in Eq. (4) of Ref. [21].

Factoring out the exact LO top quark mass dependence as in Eq. (1) is a common practice. In what follows, by the "infinite top quark mass approximation" we mean that only the quantities $\Delta_{ij}^{(k)}$ are evaluated for $M_t \to \infty$, but $\hat{A}_{\rm LO}$ remains exact in M_t.

At the LO only $\Delta_{gg}^{(0)}$ is different from zero and given by

$$\Delta_{gg}^{(0)} = \delta(1-x). \tag{3}$$

At the NLO the functions $\Delta_{gg}^{(1)}$, $\Delta_{qg}^{(1)}$ and $\Delta_{q\bar{q}}^{(1)}$ are not zero, and at the NNLO one has to consider all five contributions: $\Delta_{gg}^{(2)}$, $\Delta_{qg}^{(2)}$, $\Delta_{q\bar{q}}^{(2)}$, $\Delta_{qq}^{(2)}$, and $\Delta_{qq'}^{(2)}$.

The first results on the ρ dependence of NNLO cross sections appeared in Refs. [21] and [22], where the virtual part of $\Delta_{gg}^{(2)}$ was evaluated to $\mathcal{O}(\rho^4)$ and $\mathcal{O}(\rho^2)$, respectively. In this paper we adhere to the notations of Ref. [21]; in particular, we use $\alpha_s^{(5)}$ and the on-shell top quark mass.

[1] It is understood that ghosts are always considered together with gluons.

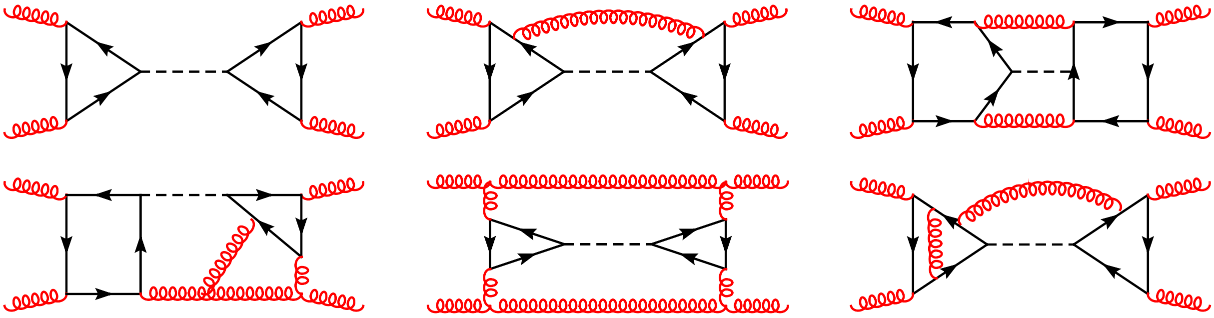

Figure 1: Sample forward scattering diagrams whose cuts correspond to the LO, NLO and NNLO corrections to $gg \to H$. Dashed, curly and solid lines represent Higgs bosons, gluons and top quarks, respectively.

Since at the LO only the virtual contribution is present, we do not discuss it further. In order to evaluate the real corrections to $\Delta_{ij}^{(k)}$, we exploit the optical theorem and compute the imaginary part of the four-point amplitudes $ij \to ij$. At NLO and NNLO this requires the evaluation of three- and four-loop diagrams, respectively. Some sample diagrams are shown in Fig. 1. Note that only the cuts dissecting the Higgs boson propagator and one or two massless lines need to be included.

We generate the diagrams with the help of `QGRAF` [23] supplemented by additional scripts that eliminate the vanishing graphs. At the next step we apply the asymptotic expansion (see, e.g., Ref. [24]) in the limit $M_t^2 \gg \hat{s}, M_H^2$, implemented in two independent programs: `q2e`/`exp` [25, 26], and an in-house Perl implementation.

This procedure factorizes the original triple-scale forward scattering functions into massive vacuum integrals (with a single scale M_t) up to three loops, that can be evaluated with `MATAD` [27], and four-point one- and two-loop integrals dependent on $\hat{s}$ and M_H. After the reduction performed with the Laporta algorithm [28, 29] we arrive to a set of master integrals that have been studied in Ref. [10] (Appendix B). Unfortunately, that reference contains a number of misprints. We independently evaluated these integrals by a combination of soft expansion[2] and differential equation methods (a detailed comparison to be provided elsewhere).

Using these techniques we have been able to compute NNLO contributions through $\mathcal{O}(\rho^2)$ for the channels gg and qg, and through $\mathcal{O}(\rho^3)$ for $q\bar{q}$, qq and qq'.

2.2 NLO results

The integral representation of the NLO corrections to the partonic cross section can be found in Refs. [6, 7]. In analytic form the ρ^0 and ρ^1 terms (gg channel) were presented in Refs. [7] and [30], respectively. In Ref. [1] terms up to $\mathcal{O}(\rho^3)$ have been demonstrated.

[2]We acknowledge help with cross checks of the soft expansion by Robert Harlander and Kemal Ozeren.

Here it is convenient for us to include terms through $\mathcal{O}(\rho^4)$ given by

$$
\begin{aligned}
\Delta_{gg}^{(1)} &= -\frac{11}{2}(1-x)^3 + 6\ \mathrm{H}(0;x)\left(2x - x^2 + x^3 - \frac{1}{1-x}\right) + 12\ \mathrm{H}(1;x)\left(2x - x^2 + x^3\right) \\
&+ \delta(1-x)\left(\frac{11}{2} + \pi^2\right) + 12\left[\frac{\ln(1-x)}{1-x}\right]_+ + \rho\left(-\frac{3x}{20} + \frac{3x^2}{20} + \frac{34}{135}\delta(1-x)\right) \\
&+ \rho^2\left(\frac{37}{11200x^2} + \frac{39}{11200x} - \frac{159}{11200} + \frac{151x}{11200} - \frac{17x^2}{2800} + \frac{3553}{113400}\delta(1-x)\right) \\
&+ \rho^3\left(\frac{23}{12000x^3} - \frac{41}{10500x^2} + \frac{1163}{288000x} - \frac{2267}{672000} + \frac{1073x}{336000} - \frac{377x^2}{201600}\right. \\
&+ \left.\frac{917641}{190512000}\delta(1-x)\right) + \rho^4\left(\frac{3347}{77616000x^4} + \frac{72587}{141120000x^3}\right. \\
&- \frac{16912657}{12418560000x^2} + \frac{58831963}{37255680000x} - \frac{2097223}{1774080000} + \frac{10057661x}{12418560000} \\
&- \left.\frac{749741x^2}{1862784000} + \frac{208588843}{251475840000}\delta(1-x)\right)\,, \qquad (4)
\end{aligned}
$$

$$
\begin{aligned}
\Delta_{qg}^{(1)} &= -1 + 2x - \frac{x^2}{3} - \frac{4 - 4x + 2x^2}{3}\left(\mathrm{H}(0;x) + 2\mathrm{H}(1;x)\right) \\
&+ \rho\left(-\frac{22}{135x} + \frac{11}{45} - \frac{11x}{90} + \frac{11x^2}{270}\right) \\
&+ \rho^2\left(\frac{3487}{259200x^2} - \frac{481}{12600x} + \frac{5171}{151200} - \frac{859x}{64800} + \frac{457x^2}{120960}\right) \\
&+ \rho^3\left(-\frac{539}{324000x^3} + \frac{98591}{15552000x^2} - \frac{15751}{1701000x} + \frac{54857}{9072000} - \frac{5357x}{2721600}\right. \\
&+ \left.\frac{7861x^2}{15552000}\right) + \rho^4\left(\frac{107369}{436590000x^4} - \frac{80543}{68040000x^3} + \frac{219381011}{95800320000x^2}\right. \\
&- \left.\frac{286017499}{125737920000x} + \frac{717887}{609638400} - \frac{889451x}{2661120000} + \frac{159415681x^2}{2011806720000}\right)\,, \qquad (5)
\end{aligned}
$$

$$
\begin{aligned}
\Delta_{q\bar{q}}^{(1)} &= \frac{32}{27}(1-x)^3 + \rho\left(\frac{88}{405x} - \frac{88}{135} + \frac{88x}{135} - \frac{88x^2}{405}\right) \\
&+ \rho^2\left(\frac{3487}{85050x^2} - \frac{9619}{85050x} + \frac{529}{5670} - \frac{961x}{85050} - \frac{421x^2}{42525}\right) \\
&+ \rho^3\left(\frac{49}{6075x^3} - \frac{107209}{5103000x^2} + \frac{2006}{127575x} - \frac{1511}{850500} + \frac{8x}{91125} - \frac{5573x^2}{5103000}\right) \\
&+ \rho^4\left(\frac{107369}{65488500x^4} - \frac{40252}{9823275x^3} + \frac{912689}{317520000x^2} - \frac{2390203}{8573040000x}\right. \\
&- \left.\frac{837833}{31434480000} + \frac{270467x}{6286896000} - \frac{7256033x^2}{47151720000}\right)\,. \qquad (6)
\end{aligned}
$$

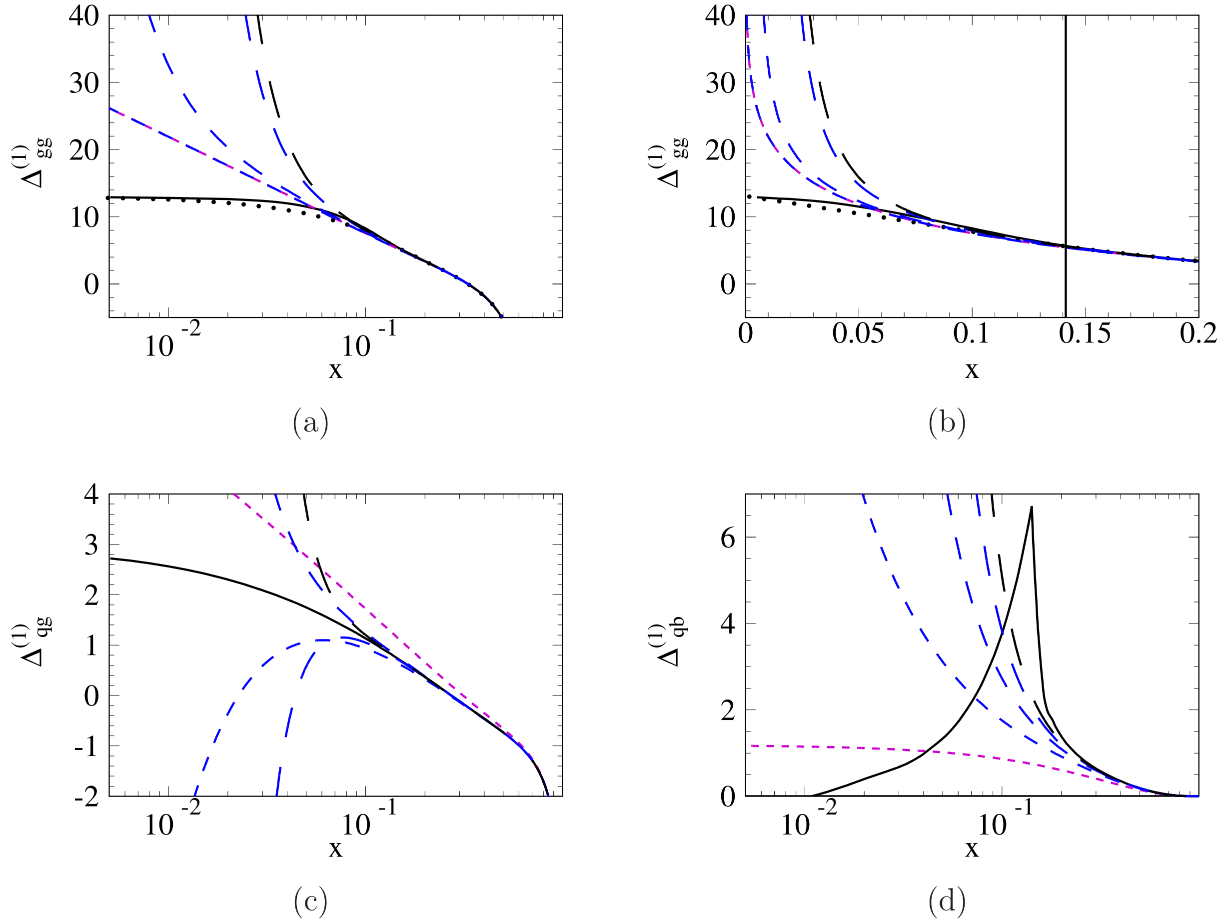

Figure 2: Partonic NLO cross sections for the (a) gg, (c) qg and (d) $q\bar{q}$ channel as functions of x for $M_H = 130$ GeV. The expansion in $\rho \to 0$ (dashed lines) is compared with the exact result (solid lines). Lines with longer dashes include higher order terms in ρ. The interpolation (see text) is shown as a dotted line. In order to demonstrate the smallness of the region below threshold we show in (b) the result for the gg channel using the linear x-scale. The vertical line at $x = M_H^2/(4M_t^2) \approx 0.14$ indicates the threshold for top quark pair production.

In Fig. 2 functions $\Delta_{ij}^{(1)}$ in the three channels are shown depending on x, evaluated for $M_H = 130$ GeV and $M_t = 173.1$ GeV [31], including successively higher orders in ρ (dashed lines). The exact result is plotted as a solid line. One sees that the leading term in ρ is smooth and demonstrates a reasonably good agreement with the exact curve.[3] However, the higher order terms in ρ introduce divergences at $x \to 0$ which are the most severe for the $q\bar{q}$ channel. This signifies the breakdown of the assumption that $M_t^2 \gg \hat{s}$ for large $\hat{s}$. Note, however, the decent convergence above the threshold for the top quark

[3] For $q\bar{q}$ the agreement is not that obvious, however, the hadronic results have the proper order of magnitude.

pair production, i.e., for $x > x_{th} = M_H^2/(4M_t^2)$.

In order to reduce the dependence on unphysical divergences near $x = 0$ at the NNLO, where exact cross sections are not known, we here devise two practical recipes and test them against the NLO results.

For the quark channels no information beyond ρ expansion is available. Thus, considering that these contributions are numerically suppressed and that x_{th} limits the applicability of our asymptotic expansion, we use the following

> Option 1:
> For $x > x_{th}$, we use the complete result including all known $\mathcal{O}(\rho^n)$ corrections, and for $x < x_{th}$ the infinite top mass approximation.

As will be demonstrated in the following section, this introduces an error in the hadronic results that is $< 50\%$, which, if also true at the NNLO, has a sufficiently small effect on the hadronic cross section compared to the overall scale uncertainty.

For the primary production channel, $gg \to H$, NLO and NNLO asymptotics near $x \to 0$ have been found in Ref. [19]. Also, NLO plots suggest that in this channel there are no pronounced threshold effects at $x = x_{th}$. Thus, here we can use a more educated

> Option 2:
> Complete $\mathcal{O}(\rho^n)$ result is matched at some point $x_m < x_{th}$ to a function $3C_1 + ax$ (NLO) or $-9C_2 \ln x + b$ (NNLO), where coefficients C_1 and C_2 are tabulated in Ref. [19] and a, b and the matching point x_m are chosen to provide the most "natural" smooth behaviour of the function.

Note that this recipe is different from the procedures suggested in Ref. [19] and Ref. [1]. The reason is that our results (as in Eq. (4)) contain genuine $1/x^n$ poles in $\mathcal{O}(\rho^n)$ contributions that are not present in the infinite top mass result used in Ref. [19] and are masked by the soft expansion of Ref. [1].

We found that an x_m such that the function and its first derivative match smoothly is a good choice at the NLO; at the NNLO, matching at $x_m = x_{th}/4$ produces reasonable results for 110 GeV $\leq M_H \leq$ 300 GeV and is consistent with the region of x where higher $\mathcal{O}(\rho^n)$ corrections demonstrate good convergence. By varying the constants and interpolating function shapes we have checked that the dependence of the hadronic cross section on the exact details of the matching procedure is quite small and that only the asymptotics near $x \to 0$ are important.

In Figs. 2 (a) and (b) the thus obtained NLO extrapolation in the gg channel is shown as a dotted line. One observes very good agreement with the exact curve, and the difference in the hadronic cross sections is negligible.

2.3 NNLO corrections

Combining the virtual part of $\Delta_{gg}^{(2)}$ calculated in Refs. [21,22] with the real contributions we arrive at the $\mathcal{O}(\rho^n)$ corrections to the quantities $\Delta_{ij}^{(2)}$ for $n = 0, 1, 2$ for gg and qg reactions, and $n = 0, 1, 2, 3$ for the remaining channels. Our results expressed in terms of harmonic polylogarithms are quite lengthy and can be obtained from the authors on request. The $\mathcal{O}(\rho^0)$ terms exactly reproduce the expressions found in Ref. [10]. Expanding the higher $\mathcal{O}(\rho^n)$ corrections in $(1-x) \ll 1$ we find complete agreement with Ref. [1].

In Fig. 3 we present non-singular parts of the functions $\Delta_{ij}^{(2)}$ for $ij = gg, qg, q\bar{q}, qq, qq'$ as functions of x. Here one can observe a behaviour similar to that at the NLO: the higher order terms in ρ develop more severe singularities near $x \to 0$, however, below the threshold the results converge. The dotted curves in Figs. 3(a) and (b) demonstrate the "Option 2" extrapolations described above. The further numerical analysis is based on these extrapolations.

3 Hadronic cross section

The hadronic cross sections are given by the convolution of the partonic cross section $\hat{\sigma}_{ij\to H+X}$ with the corresponding parton distribution functions (PDFs), which is conventionally written as follows:[4]

$$\sigma_{pp'\to H+X}(s) = \sum_{k,l\in\{g,u,\ldots,b,\bar{u},\ldots,\bar{b}\}} \int_{M_H^2/s}^{1} \mathrm{d}\tau \left[\frac{\mathrm{d}\mathcal{L}_{kl}}{\mathrm{d}\tau}\right](\tau,\mu_F)\, \hat{\sigma}_{kl\to H+X}(\hat{s}=\tau s,\mu_F)\,, \quad (7)$$

where $\mathrm{d}\mathcal{L}_{kl}/\mathrm{d}\tau$ is the so-called luminosity function given by

$$\left[\frac{d\mathcal{L}_{kl}}{d\tau}\right](\tau,\mu_F) = \int_0^1 \mathrm{d}x_1 \int_0^1 \mathrm{d}x_2\, f_{k/p}(x_1,\mu_F) f_{l/p}(x_2,\mu_F)\, \delta(\tau - x_1 x_2)\,. \quad (8)$$

For the further discussion we adopt a slightly different parametrization in terms of the "natural" parameter $x = M_H^2/\hat{s}$ and the distinct production channels:

$$\sigma_{pp'\to H+X}(s) = \sum_{ij\in\{gg,\ qg,\ q\bar{q},\ qq,\ qq'\}} \int_{M_H^2/s}^{1} \mathrm{d}x \left[\frac{\mathrm{d}\mathcal{L}_{ij}}{\mathrm{d}x}\right](x,\mu_F)\, \hat{\sigma}_{ij\to H+X}(x,\mu_F)\,, \quad (9)$$

with the straightforward modifications to the corresponding weights. For example, the

[4]In this paper we concentrate on pp collisions at the LHC peak energy $\sqrt{s} = 14$ TeV. The modifications for $p\bar{p}$ collisions at the Tevatron are obvious.

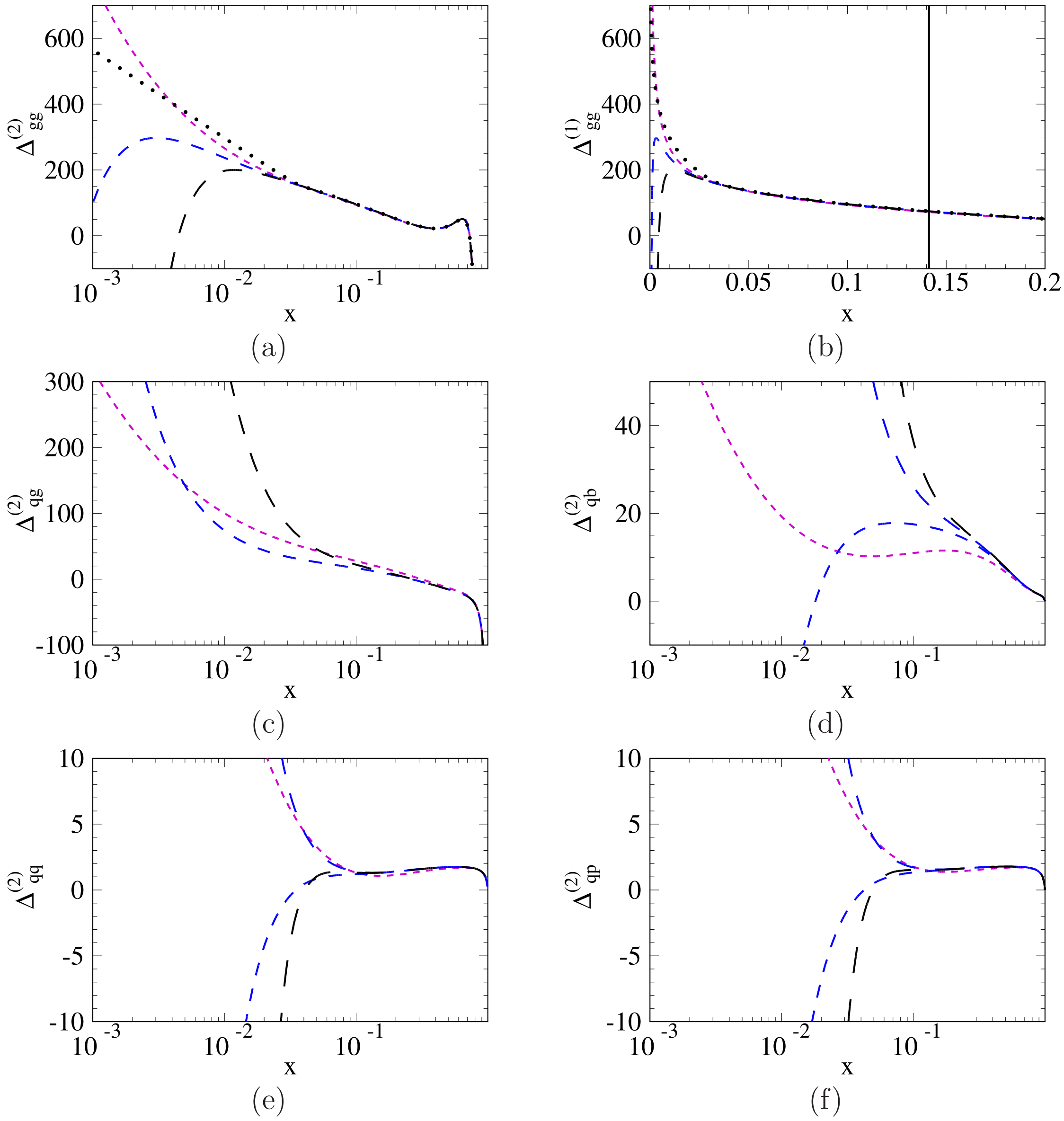

Figure 3: Partonic NNLO cross sections for the (a) gg, (c) qg, (d) $q\bar{q}$, (e) qq, (f) qq' channels functions of x for $M_H = 130$ GeV. Lines with longer dashes include higher order terms in ρ. In (b) we also show the gg channel in the linear scale. The dotted line in (a) and (b) corresponds to the matched result.

quark-gluon luminosity is defined as

$$\left[\frac{d\mathcal{L}_{qg}}{\mathrm{d}x}\right](x,\mu_F) = 2 \sum_{q\in\{u,\dots,b,\bar{u},\dots,\bar{b}\}} \int_0^1 \mathrm{d}x_1 \int_0^1 \mathrm{d}x_2\, f_{g/p}(x_1,\mu_F) f_{q/p}(x_2,\mu_F) \times\delta\left(\frac{M_H^2}{sx} - x_1 x_2\right)\frac{M_H^2}{sx^2}\,. \tag{10}$$

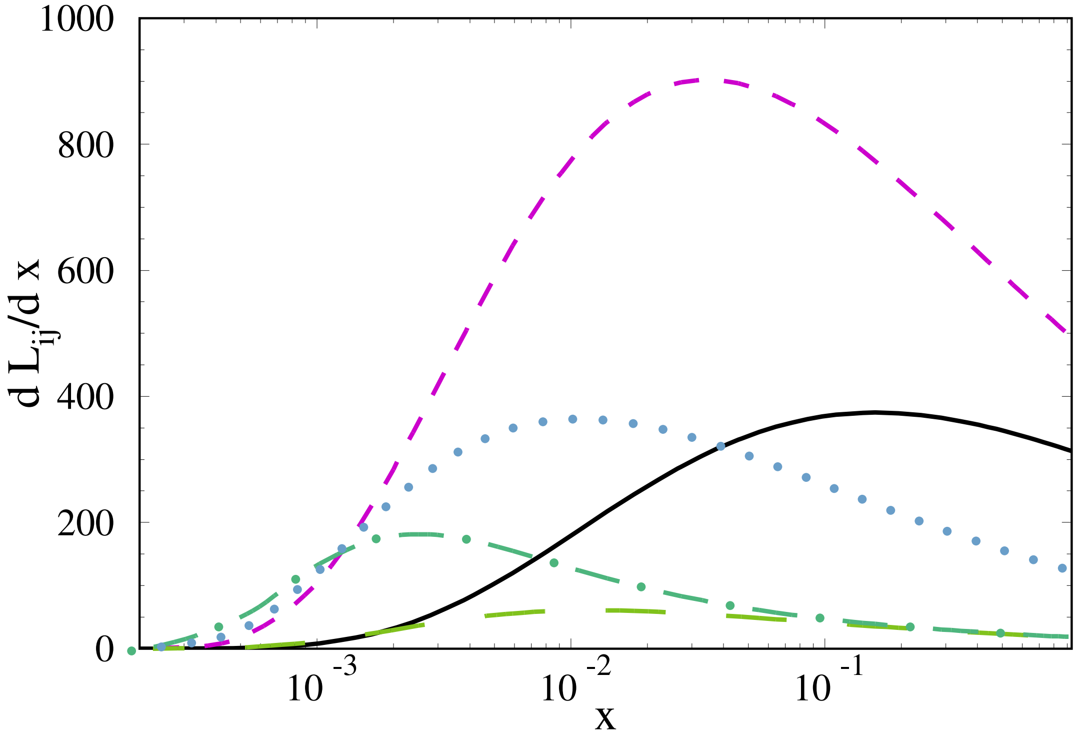

Figure 4: Luminosity functions for $ij = gg$ (solid), qg (short dashed), $q\bar{q}$ (long dashed), qq (dash-dotted), and qq' (dotted line).

For illustration we show in Fig. 4 the quantities $\mathrm{d}\mathcal{L}_{ij}/\mathrm{d}x$ for $ij = gg$, qg, $q\bar{q}$, qq, and qq'. One notices that for $x \to 0$ there is a rapid decay of all luminosity functions which is one of the main reasons that at the NLO the heavy top approximation works extremely well.

We use the parton distribution function (PDF) set MSTW2008 [32] and the α_s evolution at LO, NLO and NNLO when computing predictions to the cross section at the corresponding order. To discuss the numerical effect of our calculation we decompose the prediction of the total cross section into its LO, NLO and NNLO contributions:

$$\sigma_{pp'\to H+X}(s) \quad = \quad \sigma^{\mathrm{LO}} + \delta\sigma^{\mathrm{NLO}} + \delta\sigma^{\mathrm{NNLO}}\,, \tag{11}$$

and denote the heavy top quark approximation with an additional subscript ∞.

Let us in a first step discuss the channels involving quarks which are treated using "Option 1" as described in Section 2. In Fig. 5 we show the M_H-dependence of the NLO contribution to the hadronic cross section originating from the quantity $\Delta_{ij}^{(1)}$ (cf. Eq. (1)) normalized to the exact result as coded in HIGLU [33] for M_H between 110 GeV and 300 GeV. For the qg channel one observes that the infinite top quark mass approximation provides between 40 and 50% of the exact result. After including the ρ and ρ^2 term this

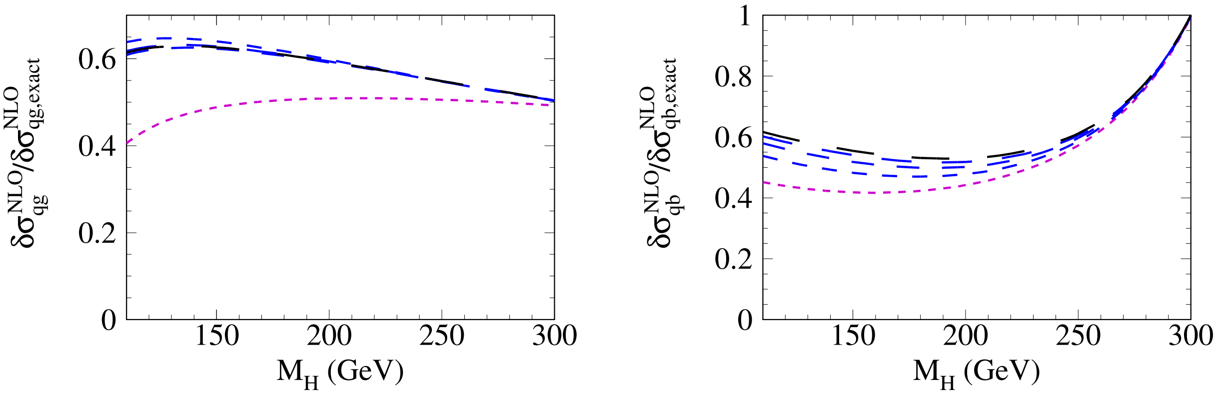

(a) (b)

Figure 5: Ratio of the NLO hadronic cross section including successive higher orders in $1/M_t$ (from short to long dashes) normalized to the exact result. (a) qg and (b) $q\bar{q}$

is improved to about 60% for the smaller Higgs boson masses whereas for $M_H = 300$ GeV the heavy top quark mass is practically unchanged. Similarly, for the $q\bar{q}$ channel we observe an improvement by about 10 to 15% for the Higgs boson masses around 140 GeV. For $M_H = 300$ GeV the heavy top expansion is practically equivalent to the exact result.

The analogous curves at NNLO can be found in Fig. 6 where we normalize the result on the infinite top quark mass approximation. In all cases the power-suppressed terms lead to an increase of the cross section between 4% and 10% for the quark-gluon and up to 25% for the quark-anti-quark channel in our range of Higgs boson masses. The very rapid convergence is observed for the qq and qq' channels where the contribution beyond the $1/M_t^2$ term is practically zero.

Let us finally turn to the numerically most important contribution, the gg channel treated with the matching to $\hat{s} \to \infty$ asymptotics denoted above as the "Option 2". In Figs. 7(a)–(c) we demonstrate the NNLO contribution to the hadronic cross section (cf. Eq. (11)) normalized to the infinite top quark mass result. The difference is that in (a), the exact LO top quark mass dependence is factored out as in Eq. (1), while in (b) the partonic cross sections both in numerator and denominator are strictly expanded in ρ. Finally, in (c) we expand $\hat{A}_{LO}$ in the numerator but keep it exact in the denominator.

For the fully expanded option (b) one observes for $M_H = 300$ GeV corrections up to 40% originating from the linear ρ term which further increase to almost 60% after including the ρ^2 term. However, when the exact leading-order top quark mass dependence is factored out (case (a)), the corrections amount to at most 8%. Considering the fact that the NNLO terms contribute about 10% of the total NNLO cross section we conclude that the top quark mass suppressed terms at NNLO alter the prediction by less than 1%. This justifies the use of the heavy top mass approximation for the evaluation of the NNLO hadronic cross section. The latter conclusion is also obtained from Fig. 7(c).

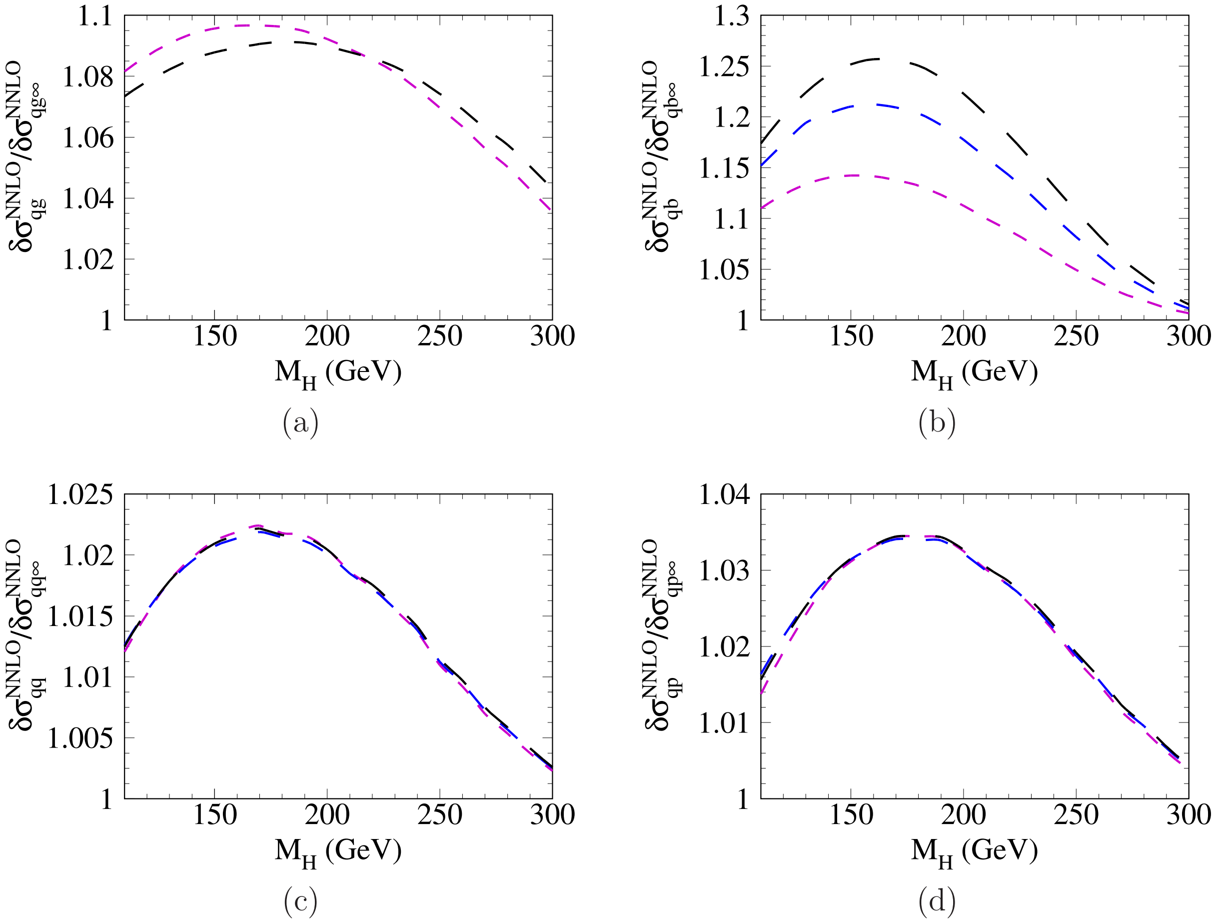

Figure 6: Ratio of the NNLO hadronic cross section including successive higher orders in $1/M_t$ (from short to long dashes) normalized to the infinite top quark mass result. (a) qg, (b) $q\bar{q}$, (c) qq, (d) qq'.

In Fig. 7(d) we also take into account the exact LO and NLO contribution and again study the effect of the different ρ terms. Similar to the case (c), we leave in the denominator the exact LO mass dependence and consider various expansion depths of the NNLO contribution in the numerator. This plot can be directly compared to the left panel of Fig. 7 in Ref. [1]. Very good agreement is observed; the minor differences can be traced back to the different matching procedures.

4 Conclusions

In this paper we present the NNLO production cross section of the Standard Model Higgs boson including finite top quark mass effects. Our calculation is based on the evaluation of the imaginary part of the forward scattering amplitudes which, via the optical theorem,

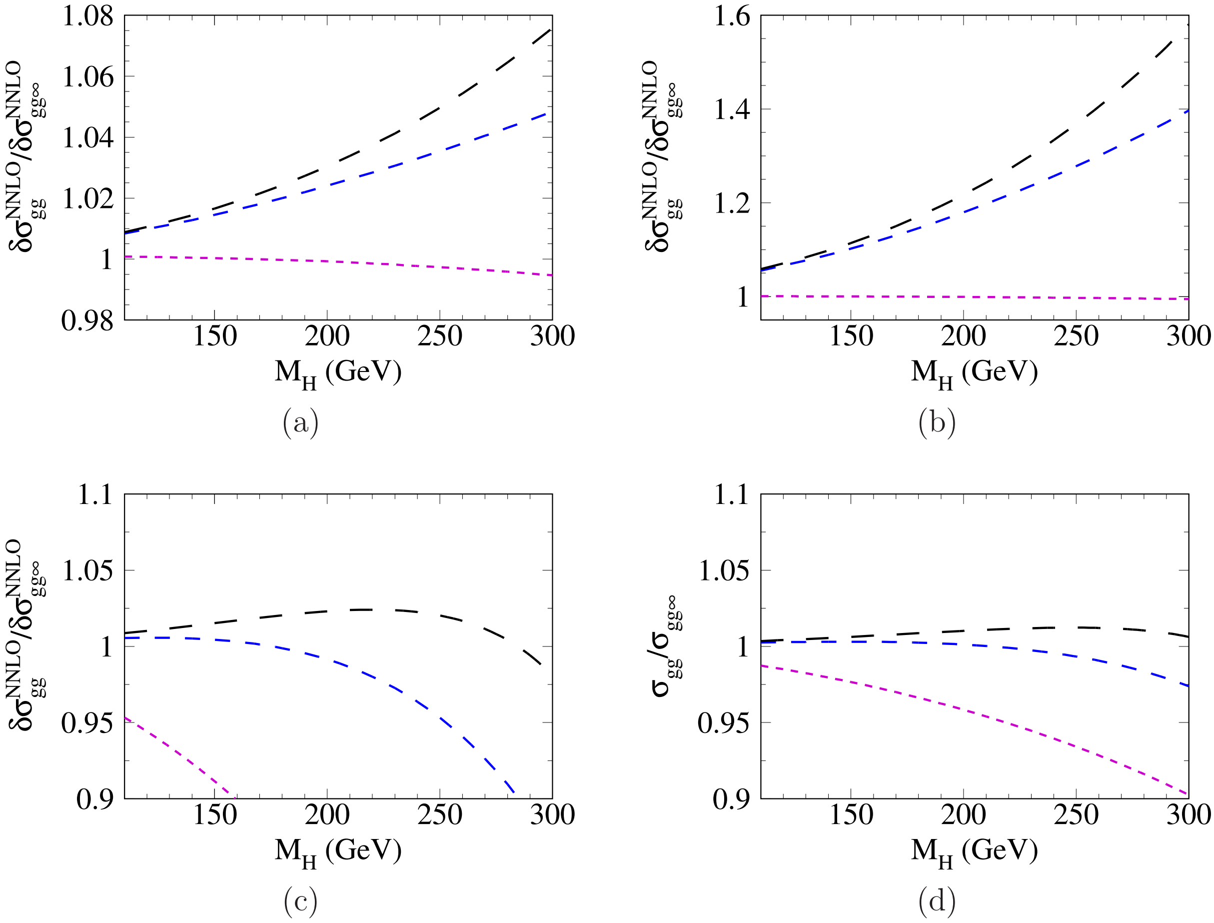

Figure 7: (a), (b) and (c): Ratio of the NNLO hadronic cross section (gg contribution) including successive higher orders in $1/M_t$ normalized to the infinite top quark mass result. In (a) the exact LO mass dependence is factorized both in the numerator and denominator. In (b) numerator and denominator are expanded in ρ, and in (c) only the numerator is expanded. (d) shows the prediction of the gluon-induced inclusive Higgs production cross section up to NNLO normalized to the heavy top limit.

directly leads to the total cross section. We apply the asymptotic expansion in order to obtain correction terms suppressed by the heavy top quark mass.

We observe rapid convergence of the series below the threshold for the production of real top quarks, i.e. for $\hat{s} \leq 4M_t^2$. However, the region of small $x = M_H^2/\hat{s}$ demonstrates $1/x^n$ singularities as a consequence of our expansion procedure. For the numerically dominant gluon-gluon channel we match our results to the large $\hat{s}$ limit, curing thus those artificial singularities and obtaining stable predictions for the hadronic cross section.

The numerical impact of the top quark mass suppressed terms is below approximately 1% and thus about a factor ten smaller than the uncertainty from scale variation. Let us, however, stress that this result was not obvious a priori. Our calculation justifies the use of the heavy top quark mass approximation when evaluating the NNLO cross section.

In addition, we confirm the results of Ref. [10] for the infinite top quark mass, and the M_t-suppressed terms calculated in Ref. [1].

Acknowledgements

We thank Robert Harlander and Kemal Ozeren for providing us with their analytical results and Kirill Melnikov for the useful communication. This work was supported by the DFG through the SFB/TR 9 "Computational Particle Physics" and by the BMBF through Grant No. 05H09VKE. M.R. was supported by the Helmholtz Alliance "Physics at the Terascale".

References

[1] R. V. Harlander and K. J. Ozeren, JHEP **11** (2009) 088, arXiv:0909.3420 [hep-ph].

[2] F. Wilczek, Phys. Rev. Lett. **39** (1977) 1304.

[3] J. R. Ellis, M. K. Gaillard, D. V. Nanopoulos and C. T. Sachrajda, Phys. Lett. B **83** (1979) 339.

[4] H. M. Georgi, S. L. Glashow, M. E. Machacek and D. V. Nanopoulos, Phys. Rev. Lett. **40** (1978) 692.

[5] T. G. Rizzo, Phys. Rev. D **22** (1980) 178 [Addendum-ibid. D **22** (1980) 1824].

[6] S. Dawson, Nucl. Phys. B **359** (1991) 283.

[7] M. Spira, A. Djouadi, D. Graudenz and P. M. Zerwas, Nucl. Phys. B **453** (1995) 17, arXiv:hep-ph/9504378.

[8] R. V. Harlander, Phys. Lett. B **492** (2000) 74, arXiv:hep-ph/0007289.

[9] R. V. Harlander and W. B. Kilgore, Phys. Rev. Lett. **88** (2002) 201801, arXiv:hep-ph/0201206.

[10] C. Anastasiou and K. Melnikov, Nucl. Phys. B **646** (2002) 220, arXiv:hep-ph/0207004.

[11] V. Ravindran, J. Smith and W. L. van Neerven, Nucl. Phys. B **665** (2003) 325, arXiv:hep-ph/0302135.

[12] R. Harlander and P. Kant, JHEP **0512** (2005) 015 [arXiv:hep-ph/0509189].

[13] K. G. Chetyrkin, B. A. Kniehl and M. Steinhauser, Nucl. Phys. B **510** (1998) 61, arXiv:hep-ph/9708255.

[14] M. Steinhauser, Phys. Rept. **364** (2002) 247, arXiv:hep-ph/0201075.

[15] R. Harlander, Eur. Phys. J. C **33** (2004) S454 [arXiv:hep-ph/0311005].

[16] S. Catani, D. de Florian, M. Grazzini and P. Nason, JHEP **0307** (2003) 028, arXiv:hep-ph/0306211.

[17] S. Moch and A. Vogt, Phys. Lett. B **631** (2005) 48 [arXiv:hep-ph/0508265].

[18] V. Ahrens, T. Becher, M. Neubert and L. L. Yang, arXiv:0809.4283 [hep-ph].

[19] S. Marzani, R. D. Ball, V. Del Duca, S. Forte and A. Vicini, Nucl. Phys. B **800** (2008) 127 [arXiv:0801.2544 [hep-ph]].

[20] D. de Florian and M. Grazzini, Phys. Lett. B **674** (2009) 291, arXiv:0901.2427 [hep-ph].

[21] A. Pak, M. Rogal and M. Steinhauser, Phys. Lett. B **679** (2009) 473 [arXiv:0907.2998 [hep-ph]].

[22] R. V. Harlander and K. J. Ozeren, Phys. Lett. B **679** (2009) 467 [arXiv:0907.2997 [hep-ph]].

[23] P. Nogueira, J. Comput. Phys. **105** (1993) 279.

[24] V. A. Smirnov, "Applied asymptotic expansions in momenta and masses," Springer Tracts Mod. Phys. **177** (2002) 1.

[25] R. Harlander, T. Seidensticker and M. Steinhauser, Phys. Lett. B **426** (1998) 125, arXiv:hep-ph/9712228.

[26] T. Seidensticker, arXiv:hep-ph/9905298.

[27] M. Steinhauser, Comput. Phys. Commun. **134** (2001) 335, arXiv:hep-ph/0009029.

[28] S. Laporta and E. Remiddi, Phys. Lett. B **379** (1996) 283, arXiv:hep-ph/9602417.

[29] S. Laporta, Int. J. Mod. Phys. A **15** (2000) 5087, arXiv:hep-ph/0102033.

[30] S. Dawson and R. Kauffman, Phys. Rev. D **49** (1994) 2298, arXiv:hep-ph/9310281.

[31] [Tevatron Electroweak Working Group and CDF Collaboration and D0 Collab], arXiv:0903.2503 [hep-ex].

[32] A. D. Martin, W. J. Stirling, R. S. Thorne and G. Watt, Eur. Phys. J. C **63** (2009) 189 [arXiv:0901.0002 [hep-ph]].

[33] M. Spira, arXiv:hep-ph/9510347.